Research Square

Preprints are preliminary reports that have not undergone peer review.
They should not be considered conclusive, used to inform clinical practice,
or referenced by the media as validated information.

Multidimensional optical encoding via light-promoted stereochemical editing

Quentin Michaudel

quentin.michaudel@chem.tamu.edu

Texas A&M University https://orcid.org/0000-0002-1791-9174

Mary Yenca

Texas A&M University

Antoine Gravet

Texas A&M University

Taeseung Hwang

Texas A&M University

Jake Nicholson

Texas A&M University

Samuel Kempel

Texas A&M University

Ting-Wei Hsu

Texas A&M University

Amanda Foster

Texas A&M University

Kaiwen Hsiao

Texas A&M University

Article

Keywords:

Posted Date: November 26th, 2026

DOI: https://doi.org/10.21203/rs.3.rs-11272215/v1

License: This work is licensed under a Creative Commons Attribution 4.0 International License.
Read Full License

Additional Declarations: There is **NO** Competing Interest.

Multidimensional optical encoding via light-promoted stereochemical editing

Mary C. Yenca, Antoine C. Gravet, Taeseung Hwang,† Jake L. Nicholson,† Samuel J. Kempel, Ting-Wei Hsu, Amanda J. Foster, Kaiwen Hsiao,* and Quentin Michaudel*

†These authors contributed equally to this work

Abstract

Information encoding/decoding in synthetic macromolecules remains in its infancy compared with the sophisticated molecular information systems found in biopolymers. Rather than emulating Nature's complex synthetic machinery through multistep iterative processes toward defined sequences, information could instead be encoded post-synthetically within a preassembled polymer. Photoresponsive materials provide an opportunity to achieve this by using light to modulate molecular structure with precise spatiotemporal resolution and generate distinct optical states for direct readout. Here, we demonstrate that main-chain *cis*/*trans* stereochemistry of poly(*p*-phenylene vinylene)s (PPVs) can serve as a continuously tunable, light-gated information state, enabling molecular information to be written with light and read through fluorescence. Divergent synthesis of electronically diverse arylated [2.2]paracyclophane-1,9-dienes (PCDs), followed by stereoretentive ring-opening metathesis polymerization (ROMP), provides all-*cis* PPV homo- and block copolymers with tunable photoisomerization kinetics, absorption, and fluorescence. An ABC triblock architecture containing a non-conjugated spacer flanked by two distinct PPV segments enables wavelength-gated *cis*-to-*trans* editing, providing multiple emissive states in solution. This stereochemical control extends to the solid state through additive-free, multicolor photopatterning using maskless digital light projection (DLP) with intensity-gated irradiation.

Main

The precise sequence of distinct repeating units in a macromolecule can encode information and dictate its properties and function, as exemplified by biopolymers such as proteins and DNA.[1,2] Achieving such molecular precision has motivated the development of elegant sequence-controlled polymerizations,[3–8] yet synthetic methods still fall short of the complexity of natural materials.[9] Accessing and reading molecular information in synthetic polymers typically requires iterative synthesis using different monomers followed by mass spectrometry decoding.[10] Intricate purification techniques such as automated chromatography[11] and molecular sieving[12] have also been used for the synthesis of discrete sequence-specific oligomers or polymers. An alternative approach would be to first synthesize a single macromolecule that can subsequently be encoded using external stimuli. Photoresponsive materials are an attractive platform for such information encoding because their optical properties are intimately linked to molecular architecture, which can be modulated with light with both spatial and temporal resolution.[13–18] Light could therefore be used to write molecular information, while fluorescence provides a direct optical readout in both solution and solid state. Such single-molecule writing ability could enable multicolor photopatterning without multicomponent blends containing several chromophores or photolithographic masks. This approach could provide a simpler route to multistate optical

information storage and patterning, with potential applications ranging from anti-counterfeiting and displays to optical information storage.[19–23]

Although photoswitchable systems including azobenzenes[24] have provided powerful approaches to structurally programmed photoresponsive materials, their reversible switching between *E*/*Z* (*trans*/*cis*) photostationary states prevents persistent molecular encoding.[25] Building on the established influence of stereochemistry on thermomechanical and optoelectronic properties of polymers,[26–31] we envisioned that irreversible *cis*-to-*trans* photoisomerization of alkene linkages[32–37] could provide persistent, stereochemically encoded optical states within a single macromolecular chromophore. More specifically, we focused on poly(*p*-phenylene vinylene) (PPV), a versatile class of conjugated polymers containing repeating photoresponsive vinylene linkages whose optical properties depend strongly on their *cis* or *trans* geometry.[38–42] PPV undergoes a unique unidirectional *cis*-to-*trans* photoisomerization, increasing polymer coplanarity while decreasing its optical band gap and solubility.[43–45] PPV also exhibits other light-mediated structural modifications that can be leveraged for photopatterning, including cross-linking and photobleaching, which permanently alter or suppress fluorescence in irradiated regions.[46–50] However, *cis*-rich PPVs predominantly absorb in the ultraviolet, limiting the use of visible light for wavelength-selective encoding.[32,37,51]

We hypothesized that extending the π-system of the *cis*-PPV backbone with electronically distinct chromophores could shift the absorption and therefore the alkene isomerization wavelengths into the visible region, enabling wavelength-gated encoding within a single macromolecule. Although aryl-substituted PPVs have been reported, these materials are typically prepared by non-stereoselective step-growth polymerizations, resulting in ill-defined polymers with low *cis* content and precluding the synthesis of complex multiblock copolymers.[39,52] We therefore targeted the synthesis of arylated PPVs by controlled chain-growth polymerization to achieve precise *cis* stereocontrol, tunable molar masses, narrow dispersities, and high chain-end fidelity, enabling the preparation of well-defined copolymer architectures. Herein, we report a diversity-oriented strategy to access electronically diverse arylated [2.2]paracyclophane-1,9-diene (PCD) monomers and their subsequent stereoretentive ring-opening metathesis polymerization (ROMP) to afford all-*cis* homo- and block copolymers with tunable photoisomerization kinetics, absorption, and fluorescence. In particular, all-*cis* 3,4-ethylenedioxythiophene (EDOT)-substituted PPV exhibited substantially redshifted absorbance and rapid photoisomerization kinetics, extending PPV photoresponsivity into the visible region up to 525 nm. Incorporation of this EDOT-substituted PPV into a three-block architecture containing a non-conjugated spacer (Fig. 1a) led to wavelength-gated *cis*-to-*trans* stereochemical editing of the PPV backbone, providing access to multiple emissive states in solution. This stereochemical editing was further leveraged to the solid state to achieve additive-free, multidimensional photopatterning using maskless digital light projection (DLP) with intensity-gated irradiation through pulse-width modulation (PWM) (Fig. 1b). Taken together, these results establish main-chain stereochemistry as a continuously tunable molecular state for writing and reading optical information, providing a general strategy for programmable photoresponsive materials at low-energy cost. By combining molecular-level information encoding with spatially and temporally resolved optical readout, this approach

provides a foundation for multistate photonic technologies[53–55] and, potentially for information-processing such as neuromorphic computing.[56]

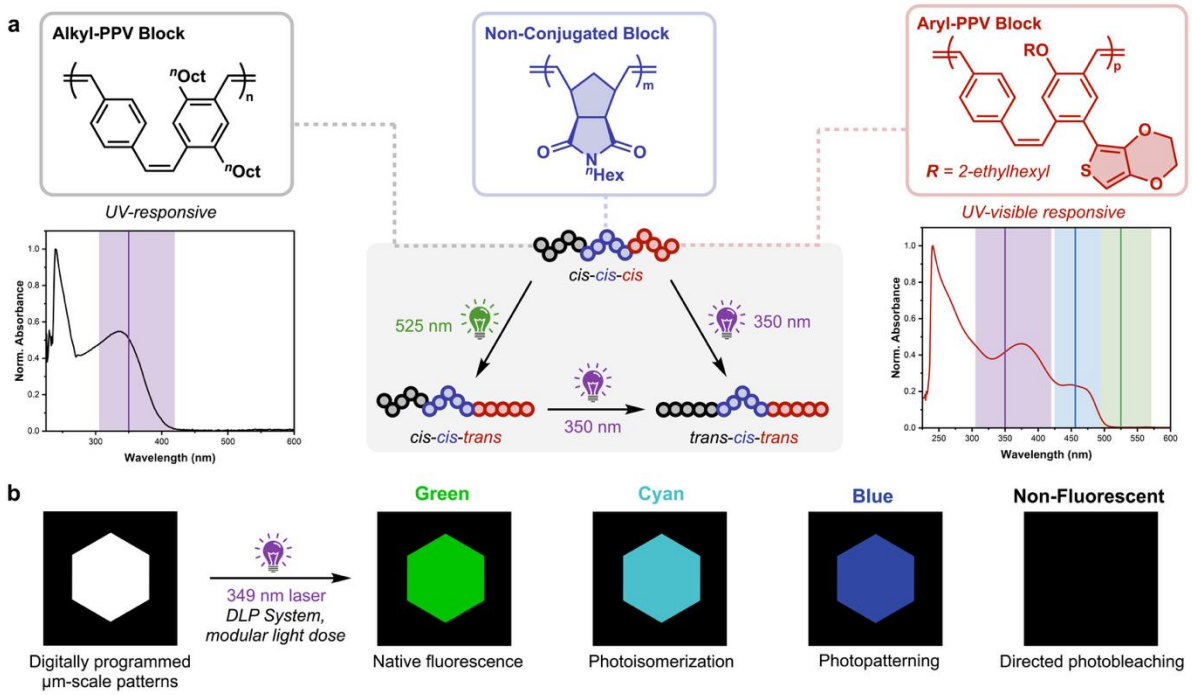

Figure 1. Wavelength-selective photoisomerization and solid-state patterning of PPV triblock copolymer.
a, Solution-state stereoblock copolymers accessed in solution state by leveraging the distinctive UV–visible absorptivity of the PPV blocks for photoisomerization. **b**, Representative solid-state emissions and photopatterning of PPV stereoblock copolymer thin films under UV irradiation of a DLP system.

Results and Discussion

Stereodefined arylated PPV synthesis

With the aim of accessing a library of all-*cis* arylated PPVs to extend absorptivity into the visible region, monotriflate PCD **1** was targeted as a synthetic branching point toward diverse PPV monomers. Instead of introducing the aryl group at the onset of the PCD construction and carrying it through several steps, **1** was prepared on gram-scale through mono-dealkylation of the diethylhexyloxy congener[57] and subsequent triflation, maintaining a solubilizing 2-ethylhexyoxy side chain to further enhance processability of the final PPV materials.[34,58] Suzuki–Miyaura cross-coupling with electronically and sterically distinct aryl groups delivered a set of six arylated monomers **M1–M6** in moderate to excellent yields using a standard set of optimized cross-coupling conditions (Fig. 2a).

Gratifyingly, **M1–M6** were shown to undergo stereoretentive ROMP[32,37] with dithiolate catalyst **Ru-St** leading to unprecedented arylated PPVs with >99% *cis* alkene contents. Following reaction optimization (Table S1), ROMP of **M1–M6** (C = 1.0 M) initiated by **Ru-St** at 40 ºC in THF in the dark afforded all-*cis* **P1–P6** with precise stereocontrol and living characteristics after 48 hours. High to quantitative conversions (88–99%) were obtained across the scope of monomers, while maintaining living characteristics (tunable M_n's, narrow $Đ$'s, and reactive chain ends, Table S1).

Impressively, strongly coordinating (benzo)thiophene-containing **P1** and **P3** both reached high conversions (88% and >99%, respectively) despite the well-documented deleterious effect of sulfur-containing groups on metathesis Ru-catalysts.[59–61] This remarkable tolerance potentially arises from the side-bound monomer approach with **Ru-St** minimizing deleterious S-coordination to the Ru carbene.[37] Importantly, perfect *cis* selectivity for each polymer was confirmed by ^{1}H NMR analysis. While UV-visible absorption spectroscopy of all-*cis* **P1–P6** in $CHCl_3$ revealed expected local maxima (λ^{max}) in the 230 and 370 nm regions of the spectra—characteristic of the $\pi \rightarrow \pi^*$ transitions of the PPV chain—EDOT-substituted **P1** exhibited an additional intense, redshifted absorption centered at 449 nm. This unique spectral feature relative to **P2–P6** is postulated to originate from resonance contribution from the electron-rich EDOT and enhanced coplanarity of this motif with the main chain.[62]

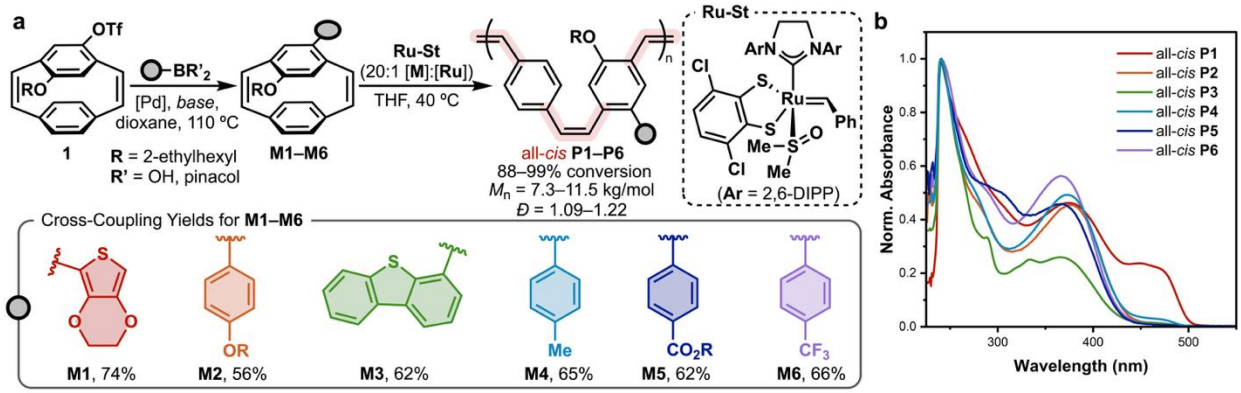

Figure 2. Divergent synthesis of stereodefined arylated PPVs via stereoretentive ROMP.
a, Suzuki–Miyaura cross-coupling of monotriflate-substituted PCD to yield diverse scope of arylated monomers, and subsequent stereoretentive ROMP to afford living all-*cis* arylated PPVs (DIPP: diisopropylphenyl). **b**, UV–visible absorption spectrum of all-*cis* arylated PPVs **P1**–**P6** with substantially enhanced redshifted absorption of all-*cis* **P1**.

Multiwavelength photoisomerization

To validate our strategy for engineering a multiwavelength-responsive PPV, we investigated the photoisomerization of **P1** in solution and compared its behavior with that of the predominantly UV-absorbing all-*cis* ^{n}octyl-substituted **P7** (Fig. 3a).[34] The distinct absorption profiles of these two polymers were intentionally selected to enable wavelength-selective control over their stereochemical states. Photoisomerization kinetics under UV, blue, and green irradiation were monitored by ^{1}H NMR spectroscopy in $CDCl_3$ for both **P1** and **P7** (Fig. 3b,c, Supplemental Fig. S8–S15). Under UV irradiation, **P1** underwent rapid and complete photoisomerization with first-order kinetics relative to alkene units, reaching 91% *trans* content within 35 min, while **P7** required 150 min to reach the same conversion. The rapid photoisomerization of **P1** is particularly promising for solution-based processing of PPVs followed by efficient photochemical transformation in device fabrication. Both all-*cis* **P1** and **P7** were successfully converted to their all-*trans* congeners following irradiation with high-intensity commercial blue LEDs (456 nm) with **P1** reaching over 70% conversion within just 10 min (Supplemental Fig. S9). The isomerization of **P7** under blue light, despite its negligible absorption at 456 nm, is likely attributable to the non-monochromatic emission of the commercial LEDs (Fig. 3a). Most importantly, the intentionally differentiated absorption profiles translated into highly orthogonal responses under green light

(525 nm): all-*cis* **P1** underwent quantitative conversion to the all-*trans* state in just over 4 h, whereas **P7** showed <3% conversion over the same period (Fig. 3d).

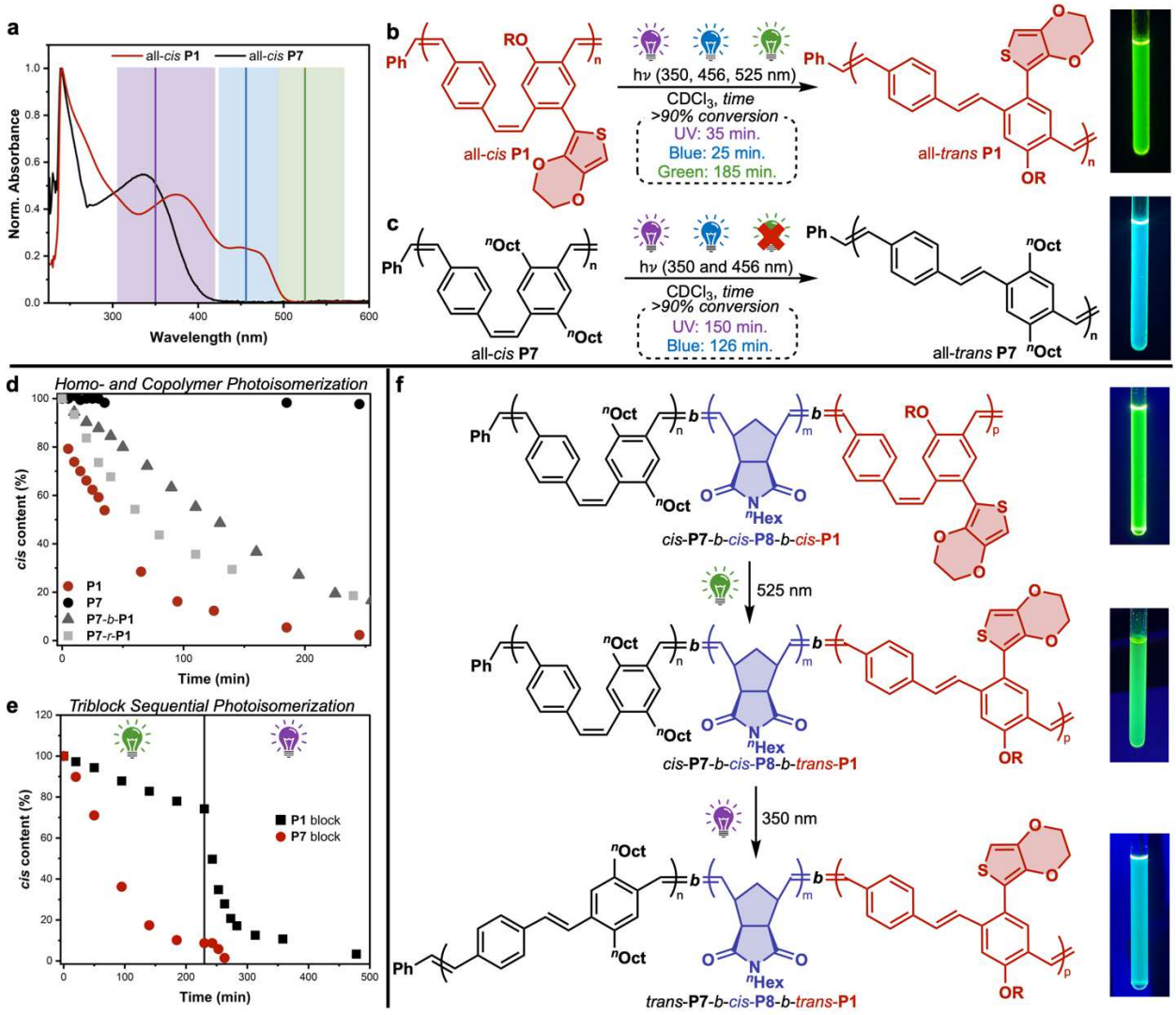

Figure 3. Architectural engineering of multiwavelength-responsive PPV systems.
a, UV–visible absorption spectrum of all-*cis* **P1** and **P7** with overlayed wavelengths and ranges of irradiation (350, 456 and 525 nm) in $CDCl_3$. **b, c**, Multi-wavelength photoisomerization of **P1** and **P7** with negligible photoreactivity exhibited by **P7** under 525 nm irradiation. **d**, Photoisomerization kinetics observing the photoreactivity of **P1** and **P7** homopolymers, **P7**-*b*-**P1** diblock copolymer, and **P7**-*r*-**P1** random copolymer. **e**, Block-specific photoisomerization kinetics of the triblock copolymer during sequential irradiation with 525 nm (0–230 min) and 350 nm (230–500 min) light. **f**, Wavelength-selective photoisomerization of the *cis*-**P7**-*b*-*cis*-**P8**-*b*-*cis*-**P1** triblock copolymer with solution-state ($CDCl_3$) fluorescence images.

Wavelength-selective copolymers

We envisioned that this marked difference in photoresponsivity could be harnessed to impart PPV block copolymers with wavelength-gated stereochemical states and, consequently, distinct fluorescence outputs, providing a simple platform for stereochemical encoding and optical readout. As an initial design, diblock *cis*-**P7**-*b*-*cis*-**P1** was synthesized by sequential monomer addition,

taking advantage of the high chain-end fidelity of the optimized stereoretentive ROMP. Size-exclusion chromatography (SEC) confirmed the formation of a well-defined block copolymer comprising segments of narrow and predictable lengths (Supplemental Fig. S1). As a benchmark, random copolymer *cis*-**P7**-*r*-*cis*-**P1** was synthesized via a one-shot synthesis using an equimolar mixture of **M1** and **M7**, which reached high and comparable conversions (Supplemental Fig. S3–4). The UV–visible absorption spectra of both copolymers displayed features characteristic of both homopolymers, with slightly increased broadening observed for the random copolymer (Supplemental Fig. S36). Interestingly, irradiation of either copolymer with green light in solution induced efficient *cis*-to-*trans* isomerization of both segments (Fig. 3d). Analysis of the individual block photoisomerization of *cis*-**P7**-*b*-*cis*-**P1** revealed >62% conversion of the **P7** segment after 4 h, compared with only 2% conversion for homopolymer **P7**, while the photoisomerization rate of the **P1** block was reduced by only ~5% relative to homopolymer **P1** (Supplemental Fig. S11, S18). These observations indicate that the **P1** block acts as an efficient antenna, enabling isomerization of the **P7** block at a wavelength where **P7** has negligible absorption. Although further studies are required to elucidate the underlying intramolecular energy/charge-transfer processes, this interblock communication reveals an antenna effect that extends the effective excitation window of PPV segments while highlighting a key challenge for their independent wavelength-selective control.

To suppress interblock communication, we inserted a non-conjugated spacer segment **P8** (Fig. 3e). Sequential stereoretentive ROMP afforded *cis*-**P7**-*b*-*cis*-**P8**-*b*-*cis*-**P1** (abbreviated as *cis*-*cis*-*cis*) with excellent control over molecular weight and dispersity, as well as complete retention of *cis* stereochemistry in each block, as confirmed by SEC, ^{1}H NMR, and DOSY NMR analyses (Supplemental Figs. S5–S6, S104–106). To our delight, the triblock copolymer exhibited pronounced wavelength selectivity: irradiation at 525 nm drove the **P1** block to >80% *trans* conversion after 140 min, while the **P7** block remained largely unreacted, reaching only 17% *trans* conversion over the same period leading to the formation of the *cis*-*cis*-*trans* triblock stereoisomer (Fig. 3f, Supplemental Fig. S22). Switching the irradiation wavelength to 350 nm dramatically altered the photoresponsiveness, rapidly driving complete photoisomerization of both blocks and affording the *trans*-*cis*-*trans* stereoblock copolymer. Importantly, the stereochemical state could be programmed sequentially using green followed by UV irradiation, providing wavelength-gated access to distinct, persistent stereochemical states within a single macromolecule.

Having established wavelength-gated and sequential control over the stereochemical states of triblock copolymer **P7**-*b*-**P8**-*b*-**P1**, we next asked whether these programmed states could be translated into distinct and readily distinguishable optical outputs. Remarkably, each successive photoisomerization event produced a nearly 10 nm hypsochromic shift in the emission maximum (Supplemental Fig. S52), progressing from green fluorescence in the *cis*-*cis*-*cis* (λ_{max}^{emi} = 495 nm) and *cis*-*cis*-*trans* (λ_{max}^{emi} = 486 nm) states to cyan fluorescence in the *trans*-*cis*-*trans* state (λ_{max}^{emi} = 478 nm). As a result, triblock **P7**-*b*-**P8**-*b*-**P1** behaves as a fluorescent "chameleon," with its emission color reflecting its programmed stereochemical state. Notably, the *cis*-*cis*-*cis* and *trans*-*cis*-*cis* states recapitulated the green fluorescence profile of **P1**, whereas the *trans*-*cis*-*trans* state exhibited the cyan fluorescence characteristic of **P7**. Thus, wavelength-selective stereochemical

editing provides access to multiple emissive states within a single polymer, with fluorescence serving as a direct optical readout of the encoded stereochemical information.

Thin film irradiation and patterning

The ability to encode stereochemical states and translate them through fluorescence suggested that these materials could serve as platforms for spatial information encoding. Accordingly, thin films of all-*cis* **P1**, all-*cis* **P7**, and all three stereoblock copolymers were evaluated using fluorescence imaging and DLP platform incorporating a digital micromirror device (DMD) for programmable light projection (Figure 4a and Supplemental Fig. S67).[63] This mask-free approach enables precise spatial control of irradiation while simultaneously modulating local light intensity through grayscale patterning controlled via PWM, providing access to a wide range of projected features varying in size, complexity, and photochemical dose. Thin films were prepared by spin-coating and mounted within an inert-atmosphere imaging chamber (Supplemental Fig. S66). Initial low-intensity irradiation with a 349 nm laser enabled visualization of the solid-state fluorescence of each polymer (Fig. 4b). While the fluorescence of all-*cis* **P1** remained consistent with its green solution-state emission, all-*cis* **P7** exhibited a marked shift from its characteristic cyan fluorescence to yellow-orange emission in the solid state, presumably reflecting differences in polymer aggregation, as reported for other PPVs.[64] In contrast, the stereoblock copolymers retained solid-state emission profiles closely matching their solution-state behavior, including the pronounced blueshift of the *trans*-*cis*-*trans* stereoblock copolymer (Supplemental Fig. S57–58). These results establish that the stereoblock architecture preserves the desired optical readout in the solid state, providing a foundation for spatially programmable fluorescence.

We next sought to translate these molecularly encoded emissive states into spatially defined fluorescence patterns using DLP. Because in such setup irradiation and fluorescence readout occur simultaneously, blue-(445 nm) or green-light (532 nm) excitation would interfere with the green/cyan emission used to read the encoded states. We therefore used the 349 nm UV laser, which provides efficient photoisomerization while remaining spectrally separated from the visible fluorescence readout. Importantly, DLP introduced a second mode of photochemical control, complementing the wavelength-gated response observed in solution with intensity-gated control of the solid-state transformation through grayscale modulation of the projected light. Irradiation of a hexagonal pattern with 80 mW of optical power produced a rapid transition from the native green-emissive state to a darker blue-emissive state, with complete pattern development within 5 min and features smaller than 300 μm^2 (Fig. 4b, Supplemental Fig. S60). A transient cyan-emissive state was observed during irradiation, consistent with the *trans*-*cis*-*trans* stereoblock copolymer based on its characteristic emission profile (Fig. 4b,d). The subsequent emergence of the blue-emissive state may arise from interchain photocrosslinking or photooxidation following photoisomerization, as previously reported for related PPV.[49] Additionally, a green halo was observed surrounding the projected features that is attributed to the scattering and internal reflection of the PPV film excited by the attenuated UV light within the asymmetric slab (argon/PPV film/coverslip). Importantly, the projected features remained spatially well-defined, demonstrating that this effect does not preclude effective pattern formation. Thus, DLP patterning of *cis*-**P7**-*b*-*cis*-**P8**-*b*-*cis*-**P1** thin films combines wavelength-gated molecular switching with

intensity-gated spatial control, enabling multidimensional fluorescence encoding within a single polymer matrix.

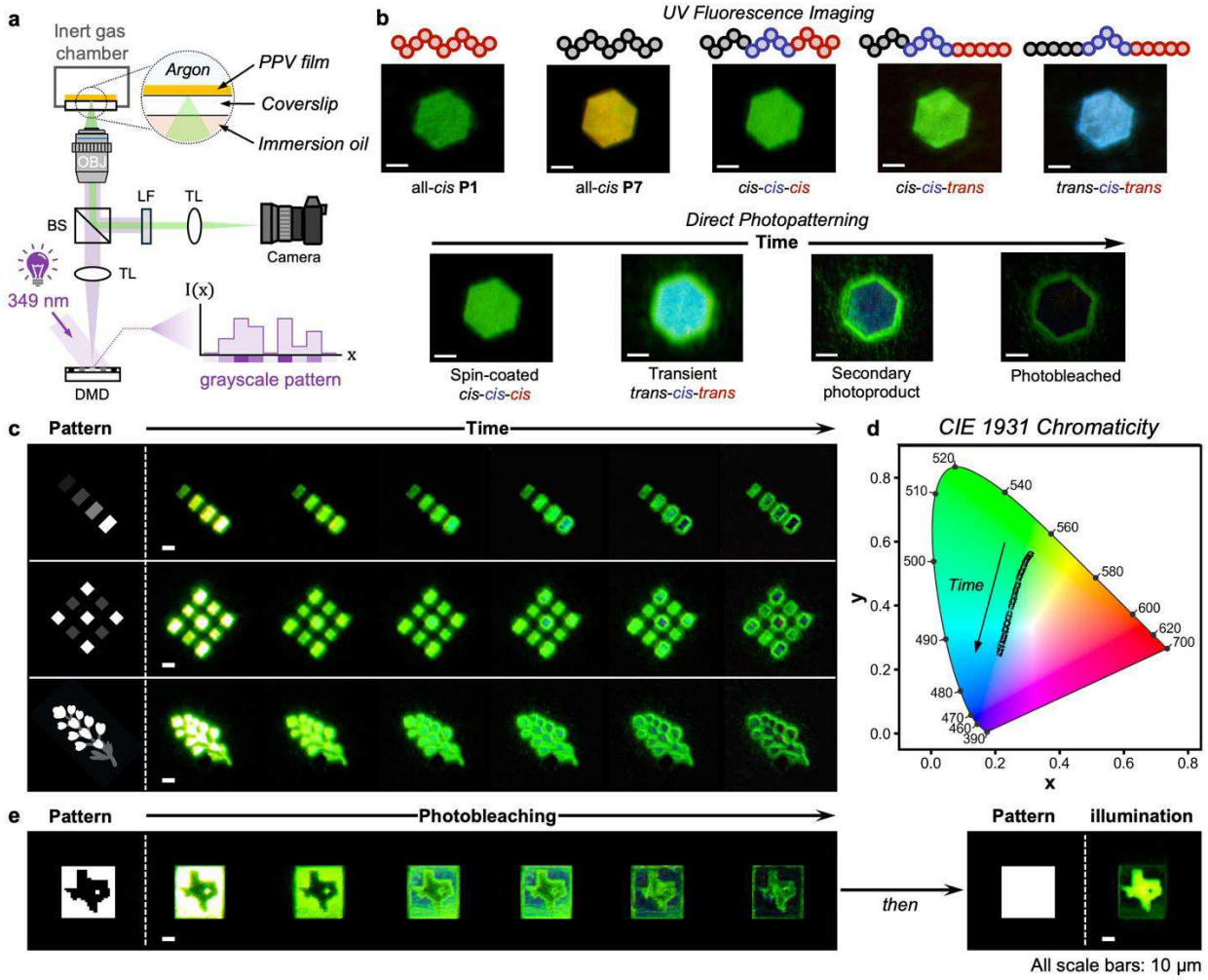

Figure 4. Dose-dependent thin film UV photopatterning.
a, Schematic image of simplified DLP platform employed for maskless photopatterning of PPV triblock thin films (TL: tube lens, BS: beam splitter, LF: long-pass filter, OBJ: objective lens). **b**, Fluorescence imaging of all-*cis* **P1**, all-*cis* **P7**, and each stereoblock copolymer; photoproducts observed over time during direct photopatterning of the *cis-cis-cis* stereoblock copolymer. **c**, Selected pattern designs (see Supporting Information for design dimensions) with varying grayscale intensities employed using 80 mW power UV irradiation over time. **d,** Time-resolved CIE 1931 chromaticity coordinates extracted color from **Fig. 4c**. **e**, Photobleaching induced negative photopatterning by sequential inverse pattern using high UV power (150 mW) followed by pattern illumination by UV power (40 mW).

Building on this multidimensional control, we next explored the limits of spatial and dose-dependent patterning using increasingly complex irradiation schemes. Grayscale designs spanning 10–100% projected intensity produced patterns with high fidelity, including a two-step grayscale grid pattern containing 25 μm^2 features (Fig. 4c, Supplemental Fig. S61–63). To quantify the color change, the fluorescence emission colors were extracted at a fixed point (Supplemental Fig. S68) for 160 seconds and the acquired fluorescence emission spectrum was projected to the CIE 1931 color space through conversion to CIE 1931 chromaticity coordinates (x, y) (Fig. 4d).[65–67] The

emission started in the green region at (x, y) = (0.311, 0.560) and blue shifted to (x, y) = (0.216, 0.261). This demonstrates that progressive stereochemical editing can be monitored as a continuum spanning two emissive states distinguishable to the human eye. Importantly, we identified a lower threshold for photochemical transformation: patterns projected at ≤ 20% grayscale intensity exhibited little to no emissive-state conversion even upon extended irradiation, instead simply illuminating the patterned region while preserving the native green-emissive state of the film. The film versatility and preservation at low dosage was demonstrated using the dynamic video-pattern-mode of DMDs (Supplementary video). This light-dose dependence enables both passive visualization and active photochemical transformation within the same material.

We further explored whether the responsiveness of the PPV material could be tuned by varying UV light intensity to deliberately induce photobleaching. Taking advantage of the known susceptibility of PPVs to high-dose UV irradiation,[46,68] selected regions of the film were exposed to an inverse Texas-shaped pattern at the highest laser power (150 mW), resulting in complete loss of fluorescence within the irradiated domains (Fig. 4e). Subsequent wide-field illumination at lower power (40 mW) revealed the persistent green-emissive film surrounded by the photobleached regions, generating a negative photopattern. Notably, the irradiated regions passed through the blue-emissive state before complete fluorescence loss, consistent with photochemical transformation preceding photobleaching. Together, these experiments demonstrate that a single triblock copolymer film can encode persistent green-emissive, blue-emissive, and non-emissive states through irradiation dose alone, providing a simple means of spatially defining multilevel molecular information with a directly accessible optical readout.

Conclusion

In summary, we developed a stereocontrolled platform for programming the structure, photochemical response, and optical output of aryl-functionalized PPVs. Divergent monomer synthesis combined with stereoretentive ROMP provided a family of well-defined all-*cis* aryl PPVs, revealing how aryl substitution can be used to tune light absorption and photoisomerization. These insights led to the design of an ABC triblock architecture in which electronically decoupled PPV segments undergo wavelength-selective, solution-phase sequential stereochemical editing, providing multiple persistent stereochemical states with distinct fluorescence signatures. In the solid state, DLP translated this molecular encoding into spatially defined fluorescence patterns, while irradiation dose introduced an additional dimension of control over emissive and non-emissive states. Together, these results demonstrate the potential of PPV *cis/trans* stereochemistry as a continuously tunable information-bearing single macromolecule, with its state written through light and read through fluorescence. Increasingly complex multiblock architectures could expand the number of independently programmable stereochemical states and enable more complex information encoding.

Methods

General Reagent Information: All reactions were carried out under an inert nitrogen atmosphere with dry solvents under anhydrous conditions unless otherwise stated. Dry dichloromethane (DCM), diethyl ether (Et_2O), tetrahydrofuran (THF), and toluene (PhMe) were obtained by passing the previously degassed solvents through activated alumina columns. Anhydrous and degassed

1,4-dioxane was purchased from Thermo Scientific Chemicals as acroseal bottle. Anhydrous THF was degassed via "freeze-pump-thaw" before being brought into a nitrogen-filled glove box. Synthesis of polymers using stereoselective ruthenium catalysts were carried out in a nitrogen-filled glove box (SG1800/750TS-F, VIGOR). Reagents were purchased at the highest commercial quality and used without further purification, unless otherwise stated. Catalyst **Ru-St** was generously donated by Umicore. Yields refer to chromatographically and spectroscopically (^{1}H NMR) homogeneous material, unless otherwise stated. Reactions were monitored by thin layer chromatography (TLC) carried out on 250 μm SiliCycle SiliaPlate™ silica plates (F254), using UV light as the visualizing agent. Flash silica gel chromatography was performed using SiliCycle SiliaFlash® Irregular Silica Gel (60 Å, particle size 40–63 μm). The polymer was isolated after precipitation using an Eppendorf 5804 centrifuge. Visible light photoisomerization was carried out using Kessil lamp models PR160L-456 nm (55W) and PR160L-525 nm (45W). Thin film spin coating was carried out using a spin coater(WS-400BZ-6NPP/LITE, Laurell).

General Analytical Information: All polymer samples were analyzed using a Tosoh EcoSec HLC 8320GPC system with a TSKgel SuperHM-M column and a TSKgel SuperH-RC column at a flow rate of 0.40 mL/min at 40 °C. THF stabilized with BHT was used as the eluent and the number-average molecular weight (M_n), weight-average molecular weight (M_w), and dispersity ($Đ$) for the polymer were calculated from an RI chromatogram against a TSKgel polystyrene standard. NMR spectra were recorded on Bruker Avance Neo 400 and Bruker Avance 500 instruments and were calibrated using residual undeuterated solvent as an internal reference ($CHCl_3$ @ 7.26 ppm ^{1}H NMR, 77.16 ppm ^{13}C NMR). The following abbreviations were used to explain NMR peak multiplicities: s = singlet, d = doublet, dd = doublet of doublets, t = triplet, q = quartet, quin. = quintet, hep. = heptet m = multiplet, br = broad. High-resolution mass spectra (HRMS) were recorded on an Agilent LC/MSD TOF mass spectrometer by Atmospheric pressure chemical ionization (APCI) or electrospray ionization (ESI). The absorption and emission measurements were carried out in dilute chloroform solutions. Absorption spectra were collected on a Shimadzu UV-2600 UV–visible spectrophotometer using 1.0 cm path length quartz cuvettes. Fluorescence measurements were collected on a Horiba FluoroMax 4 spectrofluorometer with entrance and exit slits set to 5.0 nm and an integration time of 0.1 s

Monomer synthesis, polymerization methods, molecule characterization, spectroscopic analysis, and DLP: Detailed procedures for synthesis and material processing, as well as characterization data (spectra, chromatograms, etc.) are provided in the Supplementary Information.

Data availability

The data that support the findings of this study are available in this article and its Supplementary Information.

References

1 Lutz, J.-F., Ouchi, M., Liu, D. R. & Sawamoto, M. Sequence-Controlled Polymers. *Science* **341**, 1238149 (2013).

2 Badi, N. & Lutz, J.-F. Sequence control in polymer synthesis. *Chem. Soc. Rev.* **38**, 3383–3390 (2009).

3 Xu, C. *et al.* Regio- and sequence-controlled conjugated topological oligomers and polymers via boronate-tag assisted solution-phase strategy. *Nat. Commun.* **12**, 5853 (2021).
4 Palermo, E. F. & McNeil, A. J. Impact of Copolymer Sequence on Solid-State Properties for Random, Gradient and Block Copolymers containing Thiophene and Selenophene. *Macromolecules* **45**, 5948–5955 (2012).
5 Lawrence, J. *et al.* A Versatile and Efficient Strategy to Discrete Conjugated Oligomers. *J. Am. Chem. Soc.* **139**, 13735–13739 (2017).
6 Yu, H. *et al.* Charge Transport in Sequence-Defined Conjugated Oligomers. *J. Am. Chem. Soc.* **142**, 4852–4861 (2020).
7 Fu, C. *et al.* RAFT-mediated, visible light-initiated single unit monomer insertion and its application in the synthesis of sequence-defined polymers. *Polym. Chem.* **8**, 4637–4643 (2017).
8 Xu, H., Ye, S., Zhao, R. & Seferos, D. S. Homogeneous Synthesis of Monodisperse Sequence-Defined Conjugated Oligomers by Temperature Cycling. *Angew. Chem. Int. Ed.* **61**, e202210340 (2022).
9 Lutz, J.-F., Lehn, J.-M., Meijer, E. W. & Matyjaszewski, K. From precision polymers to complex materials and systems. *Nat. Rev. Mater.* **1**, 16024 (2016).
10 Mutlu, H. & Lutz, J.-F. Reading Polymers: Sequencing of Natural and Synthetic Macromolecules. *Angew. Chem. Int. Ed.* **53**, 13010–13019 (2014).
11 Zhang, C. *et al.* Rapid Generation of Block Copolymer Libraries Using Automated Chromatographic Separation. *J. Am. Chem. Soc.* **142**, 9843–9849 (2020).
12 Dong, R. *et al.* Sequence-defined multifunctional polyethers via liquid-phase synthesis with molecular sieving. *Nat. Chem.* **11**, 136–145 (2019).
13 Xiong, X., del Campo, A. & Cui, J. in *Smart Polymers and their Applications (Second Edition)* (eds Maria Rosa Aguilar & Julio San Román) 87–153 (Woodhead Publishing, 2019).
14 Bertrand, O. & Gohy, J.-F. Photo-responsive polymers: synthesis and applications. *Polym. Chem.* **8**, 52–73 (2017).
15 Lu, P. *et al.* Wavelength-selective light-matter interactions in polymer science. *Matter* **4**, 2172–2229 (2021).
16 Heindl, A. H. & Wegner, H. A. in *Molecular Photoswitches* 477–498 (2022).
17 Xu, F. & Feringa, B. L. Photoresponsive Supramolecular Polymers: From Light-Controlled Small Molecules to Smart Materials. *Adv. Mater.* **35**, 2204413 (2023).
18 Jeon, S. *et al.* Direct-ink-write cross-linkable bottlebrush block copolymers for on-the-fly control of structural color. *Proc. Natl. Acad. Sci.* **121**, e2313617121 (2024).
19 Duan, H., Zhang, J., Weng, Y., Fan, Z. & Fan, L.-J. Dynamic Fluorescent Anti-Counterfeiting Labels Based on Conjugated Polymers Confined in Submicron Fibrous Membranes. *ACS Appl. Mater. Interfaces* **14**, 32510–32521 (2022).
20 Page, Z. A. *et al.* Novel Strategy for Photopatterning Emissive Polymer Brushes for Organic Light Emitting Diode Applications. *ACS Cent. Sci.* **3**, 654–661 (2017).
21 Yanling, Z. *et al.* Organic photoresponsive materials for information storage: a review. *Adv. Photonics* **3**, 014001 (2020).
22 Hou, X. *et al.* Tunable solid-state fluorescent materials for supramolecular encryption. *Nat. Commun.* **6**, 6884 (2015).

23 Kim, S. C., Park, J. H., Chin, S. O., Kim, J. & Kim, D. Recent advances in anti-counterfeiting technology using fluorescent hybrid materials. *Adv. Compos. Hybrid Mater.* **9**, 24 (2025).

24 Sun, S., Liang, S., Xu, W.-C., Xu, G. & Wu, S. Photoresponsive polymers with multi-azobenzene groups. *Polym. Chem.* **10**, 4389–4401 (2019).

25 García-Iriepa, C., Marazzi, M., Frutos, L. M. & Sampedro, D. E/Z Photochemical switches: syntheses, properties and applications. *RSC Adv.* **3**, 6241–6266 (2013).

26 Worch, J. C. *et al.* Stereochemical enhancement of polymer properties. *Nat. Rev. Chem.* **3**, 514–535 (2019).

27 Yang, X., Gitter, S. R., Roessler, A. G., Zimmerman, P. M. & Boydston, A. J. An Ion-Pairing Approach to Stereoselective Metal-Free Ring-Opening Metathesis Polymerization. *Angew. Chem. Int. Ed.* **60**, 13952–13958 (2021).

28 Hsu, T.-W., Kempel, S. J., Felix Thayne, A. P. & Michaudel, Q. Stereocontrolled acyclic diene metathesis polymerization. *Nat. Chem.* **15**, 14–20 (2023).

29 Kempel, S. J., Hsu, T.-W., Nicholson, J. L. & Michaudel, Q. cis-Selective Acyclic Diene Metathesis Polymerization of α,ω-Dienes. *J. Am. Chem. Soc.* **145**, 12459–12464 (2023).

30 Nicholson, J. L., Gravet, A. C. & Michaudel, Q. Telechelic all-cis polycyclooctene via catalytic stereoretentive ROMP for the synthesis of polylactide-based ABA triblock copolymers. *Faraday Discuss.* **262**, 226–237 (2026).

31 Nicholson, J. L. & Michaudel, Q. Recent advances in cis/trans stereoselective polymerizations toward functional materials with tailored properties. *ChemRxiv* **2026**

32 Hsu, T. W., Kim, C. & Michaudel, Q. Stereoretentive Ring-Opening Metathesis Polymerization to Access All-cis Poly(p-phenylenevinylene)s with Living Characteristics. *J. Am. Chem. Soc.* **142**, 11983–11987 (2020).

33 Kempel, S. J., Hsu, T.-W. & Michaudel, Q. Stereoretentive Olefin Metathesis: A New Avenue for the Synthesis of All-cis Poly(p-phenylene vinylene)s and Stereo-defined Polyalkenamers. *Synlett* **32**, 851–857 (2021).

34 Hsu, T.-W., Kempel, S. J. & Michaudel, Q. All-cis poly(p-phenylene vinylene)s with high molar masses and fast photoisomerization rates obtained through stereoretentive ring-opening metathesis polymerization of [2,2]paracyclophane dienes with various aryl substituents. *J. Polym. Sci.* **60**, 569–578 (2022).

35 Michaudel, Q., Kempel, S. J., Hsu, T.-W. & deGruyter, J. N. in *Comprehensive Organometallic Chemistry IV* (eds Gerard Parkin, Karsten Meyer, & Dermot O'hare) 265–338 (Elsevier, 2022).

36 Mandal, H. *et al.* Linear and Nonlinear Optical Properties of All-cis and All-trans Poly(p-phenylenevinylene). *J. Phys. Chem. C* **128**, 2518–2528 (2024).

37 Nicholson, J. L. *et al.* Leveraging Mechanistic Insights into Stereoretentive ROMP for Precision Synthesis of Poly(p-phenylene vinylene)s. *J. Am. Chem. Soc.* **148**, 19943–19955 (2026).

38 Burroughes, J. H. *et al.* Light-emitting diodes based on conjugated polymers. *Nature* **347**, 539–541 (1990).

39 Grimsdale, A. C., Leok Chan, K., Martin, R. E., Jokisz, P. G. & Holmes, A. B. Synthesis of Light-Emitting Conjugated Polymers for Applications in Electroluminescent Devices. *Chem. Rev.* **109**, 897–1091 (2009).

40 Kulkarni, A. P., Tonzola, C. J., Babel, A. & Jenekhe, S. A. Electron Transport Materials for Organic Light-Emitting Diodes. *Chem. Mater.* **16**, 4556–4573 (2004).

41 Su, R., Park, S. H., Ouyang, X., Ahn, S. I. & McAlpine, M. C. 3D-printed flexible organic light-emitting diode displays. *Sci. Adv.* **8**, eabl8798 (2022).
42 Yu, G., Gao, J., Hummelen, J. C., Wudl, F. & Heeger, A. J. Polymer Photovoltaic Cells: Enhanced Efficiencies via a Network of Internal Donor-Acceptor Heterojunctions. *Science* **270**, 1789–1791 (1995).
43 Arai, T. & Tokumaru, K. Photochemical one-way adiabatic isomerization of aromatic olefins. *Chem. Rev.* **93**, 23–39 (1993).
44 Shin, S. *et al.* Living Light-Induced Crystallization-Driven Self-Assembly for Rapid Preparation of Semiconducting Nanofibers. *J. Am. Chem. Soc.* **140**, 6088–6094 (2018).
45 Xia, H. *et al.* Three-dimensional micronanofabrication via two-photon-excited photoisomerization. *Appl. Phys. Lett.* **95** (2009).
46 Scurlock, R. D., Wang, B., Ogilby, P. R., Sheats, J. R. & Clough, R. L. Singlet Oxygen as a Reactive Intermediate in the Photodegradation of an Electroluminescent Polymer. *J. Am. Chem. Soc.* **117**, 10194–10202 (1995).
47 Antoniadis, H. *et al.* Enhanced carrier photogeneration by defects in conjugated polymers and its mechanism. *Phys. Rev. B* **50**, 14911–14915 (1994).
48 Yan, M., Rothberg, L. J., Papadimitrakopoulos, F., Galvin, M. E. & Miller, T. M. Defect Quenching of Conjugated Polymer Luminescence. *Phys. Rev. Lett.* **73**, 744–747 (1994).
49 Deng, X. & Wong, K. Y. Cross-Linked Conjugated Polymers for Achieving Patterned Three-Color and Blue Polymer Light-Emitting Diodes with Multi-Layer Structures. *Macromol. Rapid Commun.* **30**, 1570–1576 (2009).
50 Pogantsch, A. *et al.* Tuning the Electroluminescence Color in Polymer Light-Emitting Devices Using the Thiol-Ene Photoreaction. *Adv. Funct. Mater.* **15**, 403–409 (2005).
51 Wang, F. *et al.* A solution-processible poly(p-phenylene vinylene) without alkyl substitution: Introducing the cis-vinylene segments in polymer chain for improved solubility, blue emission, and high efficiency. *J. Polym. Sci., Part A: Polym. Chem.* **46**, 5242–5250 (2008).
52 Yu, C.-Y. & Lai, Y.-C. Soluble Phenylenevinylene Polymers Containing Tetraphenylethene Units by Ring-Opening Metathesis Polymerization. *Macromol. Chem. Phys.* **219**, 1800135 (2018).
53 Yan, Z. *et al.* Decoding the future: opportunities and challenges in next-generation optical data storage [Invited]. *Chin. Opt. Lett.* **21**, 120051 (2023).
54 Corredor, C. C., Huang, Z.-L., Belfield, K. D., Morales, A. R. & Bondar, M. V. Photochromic Polymer Composites for Two-Photon 3D Optical Data Storage. *Chem. Mater.* **19**, 5165–5173 (2007).
55 Xu, T. *et al.* Organic Transistor Nonvolatile Memory with Three-Level Information Storage and Optical Detection Functions. *ACS Appl. Mater. Interfaces* **12**, 21952–21960 (2020).
56 Lamon, S., Zhang, Q., Yu, H. & Gu, M. Neuromorphic Optical Data Storage Enabled by Nanophotonics: A Perspective. *ACS Photonics* **11**, 874–891 (2024).
57 Mann, A., Wang, C., Dumlao, B. L. & Weck, M. Functionalized [2.2]Paracyclophanedienes as Monomers for Poly(p-phenylenevinylene)s. *ACS Macro Lett.* **13**, 112–117 (2024).
58 Gorman, C. B., Ginsburg, E. J. & Grubbs, R. H. Soluble, highly conjugated derivatives of polyacetylene from the ring-opening metathesis polymerization of monosubstituted

cyclooctatetraenes: synthesis and the relationship between polymer structure and physical properties. *J. Am. Chem. Soc.* **115**, 1397–1409 (2002).
59 Chang, C.-C. & Emrick, T. Functional Polyolefins Containing Disulfide and Phosphoester Groups: Synthesis and Orthogonal Degradation. *Macromolecules* **47**, 1344–1350 (2014).
60 Wagener, K. B. *et al.* Kinetics of Acyclic Diene Metathesis (ADMET) Polymerization. Influence of the Negative Neighboring Group Effect. *Macromolecules* **30**, 7363–7369 (1997).
61 Shon, Y.-S. & Lee, T. R. Catalytic ring-closing olefin metathesis of sulfur-containing species: Heteroatom and other effects. *Tetrahedron Lett.* **38**, 1283–1286 (1997).
62 Roncali, J. Molecular Engineering of the Band Gap of π-Conjugated Systems: Facing Technological Applications. *Macromol. Rapid Commun.* **28**, 1761–1775 (2007).
63 Hwang, T. & Hsiao, K. Dual-wavelength digital-light projection for precise spatial-temporal photochemical reaction-kinetics control. *Addit. Manuf.* **114**, 105021 (2025).
64 Bellacanzone, C., Otaegui, J. R., Hernando, J., Ruiz-Molina, D. & Roscini, C. Tunable Thermofluorochromic Sensors Based on Conjugated Polymers. *Adv. Opt. Mater.* **10**, 2102423 (2022).
65 CIE. Commission internationale de l'eclairage proceedings, 1931. *Cambridge University, Cambridge* (1932).
66 CIE. Colorimetry, 4th Edition. Report No. CIE 015:2018, (CIE, Vienna, Austria, 2018).
67 Kelly, K. L. Color Designations for Lights. *J. Opt. Soc. Am.* **33**, 627–632 (1943).
68 Sutherland, D. G. J. *et al.* Photo-oxidation of electroluminescent polymers studied by core-level photoabsorption spectroscopy. *Appl. Phys. Lett.* **68**, 2046–2048 (1996).

Acknowledgements
This work was supported by the National Science Foundation (CAREER 2238888 to Q.M. and CAREER 2542480 to K.H), as well as the Welch Foundation (A-2204-20240404. to Q.M. and M2403098 to K.H.). Q.M. thanks the Camille and Henry Dreyfus Foundation for support via the Camille Dreyfus Teacher-Scholar Award (TC-24-059). M.C.Y. and J.L.N. were partially supported by the Hagler Institute for Advanced Study through HEEP Graduate Fellowships. The use of the NMR Facility in the Department of Chemistry and the Soft Matter Facility (RRID: SCR_022482) at Texas A&M University is acknowledged. The authors also thank Umicore for the generous donation of metathesis catalysts.

Author information
Authors and Affiliations
Department of Chemistry, Texas A&M University, College Station, Texas, USA
Mary C. Yenca, Antoine C. Gravet, Jake L. Nicholson, Samuel J. Kempel, Ting-Wei Hsu, Amanda J. Foster, & Quentin Michaudel
Department of Materials Science and Engineering, Texas A&M University, College Station, Texas, USA
Taeseung Hwang, Kaiwen Hsiao, & Quentin Michaudel

Contributions
M.C.Y., A.C.G., T.H., J.L.N., S.J.K., T.-W.H., and A.J.F. performed the research. All authors designed the research and analyzed the data. M.C.Y., A.C.G., T.H., J.L.N., K.H., and Q.M. wrote the paper and Supplementary Information.

Corresponding authors
Correspondence to Quentin Michaudel and Kaiwen Hsiao.

Ethics declarations

Competing interests
The authors declare no competing interests.

Supplementary Files

This is a list of supplementary files associated with this preprint. Click to download.

- SIfilesdescription.docx
- SupplementaryVideo.mov
- SIPPVencoding100126.pdf